Journal of Neuroscience Methods 224 (2014) 96–106

Contents lists available at ScienceDirect

Journal of Neuroscience Methods

journal homepage: www.elsevier.com/locate/jneumeth

Basic Neuroscience

There's more than one way to scan a cat: Imaging cat auditory cortex with high-field fMRI using continuous or sparse sampling

Amee J. Hall[a,g], Trecia A. Brown[b,g], Jessica A. Grahn[c,d], Joseph S. Gati[e,f], Pam L. Nixon[b,g], Sarah M. Hughes[e], Ravi S. Menon[d,e,f], Stephen G. Lomber[b,c,d,e,g,h,*]

[a] Department of Anatomy and Cell Biology, University of Western Ontario, London, Ontario N6A 5C2, Canada
[b] Department of Physiology and Pharmacology, Schulich School of Medicine & Dentistry, University of Western Ontario, London, Ontario N6A 5C2, Canada
[c] Department of Psychology, Faculty of Social Science, University of Western Ontario, London, Ontario N6A 5C2, Canada
[d] Brain and Mind Institute, University of Western Ontario, London, Ontario N6A 5C2, Canada
[e] Centre for Functional and Metabolic Mapping, Robarts Research Institute, University of Western Ontario, London, Ontario N6A 5C2, Canada
[f] Department of Medical Biophysics, University of Western Ontario, London, Ontario N6A 5C2, Canada
[g] Cerebral Systems Laboratory, University of Western Ontario, London, Ontario N6A 5C2, Canada
[h] National Centre for Audiology, University of Western Ontario, London, Ontario N6A 5C2, Canada

HIGHLIGHTS

- Sparse and continuous fMRI methods of scanning cat auditory system are compared.
- Continuous scanning produces greater extent of activation in auditory cortex.
- No differences between scanning methods were observed in auditory midbrain.
- Magnitude of activation was greater in auditory cortex than in midbrain.
- No consistent activation was observed in auditory thalamus with either method.

ARTICLE INFO

Article history:
Received 15 July 2013
Received in revised form
19 December 2013
Accepted 20 December 2013

Keywords:
Tonal stimulation
Broadband noise
7-Tesla
Thalamus
Inferior colliculus

ABSTRACT

When conducting auditory investigations using functional magnetic resonance imaging (fMRI), there are inherent potential confounds that need to be considered. Traditional continuous fMRI acquisition methods produce sounds >90 dB which compete with stimuli or produce neural activation masking evoked activity. Sparse scanning methods insert a period of reduced MRI-related noise, between image acquisitions, in which a stimulus can be presented without competition. In this study, we compared sparse and continuous scanning methods to identify the optimal approach to investigate acoustically evoked cortical, thalamic and midbrain activity in the cat. Using a 7 T magnet, we presented broadband noise, 10 kHz tones, or 0.5 kHz tones in a block design, interleaved with blocks in which no stimulus was presented. Continuous scanning resulted in larger clusters of activation and more peak voxels within the auditory cortex. However, no significant activation was observed within the thalamus. Also, there was no significant difference found, between continuous or sparse scanning, in activations of midbrain structures. Higher magnitude activations were identified in auditory cortex compared to the midbrain using both continuous and sparse scanning. These results indicate that continuous scanning is the preferred method for investigations of auditory cortex in the cat using fMRI. Also, choice of method for future investigations of midbrain activity should be driven by other experimental factors, such as stimulus intensity and task performance during scanning.

1. Introduction

Investigations of cortical, and subcortical, processing of acoustic information using the cat have provided a foundation for many of the current theories in auditory neuroscience. However, the invasive nature of techniques used such as electrophysiological recording, makes it necessary to use alternate techniques, such as functional magnetic resonance imaging (fMRI), when conducting clinical investigations. Therefore, it would be highly beneficial to

* Corresponding author at: Brain and Mind Institute, Natural Sciences Centre, University of Western Ontario, 1151 Richmond Street North, London, Ontario N6A 5B7, Canada. Tel.: +1 519 663 5777x24110; fax: +1 519 931 5233.
E-mail address: steve.lomber@uwo.ca (S.G. Lomber).

0165-0270/$ – see front matter © 2014 Elsevier B.V. All rights reserved.
http://dx.doi.org/10.1016/j.jneumeth.2013.12.012

future investigations if literature were available using fMRI in the cat to provide a more comparable link between these experimental approaches.

The use of fMRI to study the organization of auditory cortex has inherent obstacles that must be overcome. In particular, standard blood oxygen level dependent (BOLD) fMRI acquisition techniques using single shot echo planar imaging (EPI) may produce sound pressure levels (SPLs) greater than 90 dB SPL with peak SPLs occurring at approximately 1 kHz (Amaro et al., 2002; Peelle et al., 2010; Price et al., 2001). It has also been reported that magnets of higher field strength produce significantly higher levels of noise (Moelker and Pattynama, 2003; Price et al., 2001; Ravicz et al., 2000). Therefore, the potential confound of scanner noise increases with the current trend in research toward using higher field magnets to produce higher resolution images. The acoustic noise which accompanies acquisition presents several potential problems for conducting experiments using auditory stimuli including: (1) interactions at the basilar membrane between scanner noise and the intended stimuli; (2) the masking of intended stimulus evoked neural activity by the scanner noise; and (3) the reduction in responsiveness to subsequent presented stimuli (Amaro et al., 2002; Bandettini et al., 1998; Hall et al., 1999; Peelle et al., 2010; Petkov et al., 2009; Talavage et al., 1999). In studies of human subjects, scanner noise is attenuated by employing methods such as headphones, ear inserts, and sound-absorbent material placed around the head and covering the ears (Amaro et al., 2002). These methods, however, do not eliminate scanner noise and therefore potentially still confound the acquired data.

An approach referred to as sparse scanning (Hall et al., 1999), originally introduced as clustered-volume acquisitions (Edmister et al., 1999), has been developed in an attempt to combat some of the confounds present in auditory fMRI. Sparse scanning takes advantage of the delay in the hemodynamic response to neural activity by inserting a pause between volume acquisitions. During this period, a stimulus may be presented without competition and the response to that stimulus can be recorded (Hall et al., 1999; Peelle et al., 2010). While the period between acquisitions is quieter, it would be remiss to think of it as silent. Ambient noise related to ventilation, cryogen pumping, and monitoring equipment are all present during this period and, without effective acoustic shielding, could also affect fMRI data (Moelker and Pattynama, 2003). To take advantage of this technique, the hemodynamic response function (HRF) must be defined so that acquisition is timed to take place at the peak. The HRF of auditory cortex peaks at approximately 3–5 s for humans (Backes and van Dijk, 2002; Belin et al., 1999) and monkeys (Baumann et al., 2010). The HRF has recently been defined for the cat (Brown et al., 2013) and also peaks at 3–5 s, making it possible to optimize sparse scanning for the cat.

Sparse scanning provides many advantages for the presentation of auditory stimuli. Sparse scanning samples the hemodynamic response function (HRF) at its peak potentially resulting in a greater , yet potentially with a higher degree of variability, measured BOLD response. In contrast, continuous scanning samples across the HRF providing a more stable level of measured BOLD response. Moreover, sparse scanning lacks the effects of spin history which are present during continuous scanning (Woods et al., 2009) and cortical habituation due to scanner noise is limited. However, there are also characteristics of the sparse scanning method that could be problematic. The addition of gaps in fMRI acquisition result in a lengthened trial time and reduces the number of acquired volumes during the same time period (Peelle et al., 2010). Also, the limited number of volumes leads to a reduction of the statistical power in the acquisition.

There have only been a few studies which have actively compared the two techniques to assess their optimality. Petkov et al. (2009) showed data from macaque monkeys in which sparse scanning resulted in larger activations and tonotopic mapping. This study lengthened the acquisition time (TA) of the continuous volume to more closely match the repetition time (TR) of the sparse paradigm. In doing this, several of the advantages of continuous scanning, namely the larger amount of data which can be collected in a given time period and a better resolution of the hemodynamic response, biased results toward sparse scanning. Peelle et al. (2010) conducted a comparable study in humans using a similar TA for both sparse and continuous scanning. In this study, while the sparse technique generally resulted in a higher signal, continuous scanning resulted in better statistical power. Similarly, Woods et al. (2009) also found that sparse scanning resulted in larger magnitude activations when compared to continuous scanning. However, this study noted that, beyond magnitude, both methods resulted in similar activation patterns and locations.

The present study provides a fundamental investigation of both sparse and continuous scanning methods to identify the optimal method for auditory investigations of the cat cerebrum. There have been numerous investigations of the auditory system using either sparse (Davis and Johnsrude, 2003; Langers et al., 2007; Scarff et al., 2004; van den Noort et al., 2008; Vannest et al., 2009) or continuous scanning (Inan et al., 2004; Talavage et al., 2000; Wessinger et al., 1997). Given that there are benefits and caveats to both techniques, it was not possible to predict which would be ideal for imaging acoustically evoked activity.

2. Methods

Five adult (>6 m) female domestic shorthair cats were selected for this project. All animals were obtained from a commercial laboratory animal breeding facility (Liberty Labs, Waverly, NY) and housed as a clowder. All procedures were approved by the University of Western Ontario's Animal Use Subcommittee of the University Council on Animal Care and were in accordance with the National Research Council's *Guidelines for the Care and Use of Mammals in Neuroscience and Behavioral Research* (Van Sluyters et al., 2003) and the Canadian Council on Animal Care's *Guide to the Care and Use of Experimental Animals* (Olfert et al., 1993).

2.1. Anesthesia and recovery

All animals were pre-medicated (intramuscular injection; i.m.) with a mixture of atropine (0.02 mg/kg) and acepomazine (0.02 mg/kg). This pre-medication protocol has been shown to reduce the amount of general anesthesia required (Dyson et al., 1988) and thus potentially reduce any suppressive cortical effects. After 20 min, a solution of ketamine (4 mg/kg) and dexdomitor (0.025 mg/kg) was administered (i.m.) to induce anesthesia. This anesthetic regime has been previously used and found to be effective in measuring BOLD responses in the cat (Brown et al., 2013). Once anesthetized, as determined by lack of paw-pinch or ear reflex, the animals were then intubated and an indwelling feline catheter was placed in the saphenous vein to facilitate maintenance of anesthesia. Body temperature was maintained with heating discs and vital signs were continually monitored. Each cat was then placed in a custom made Plexiglas apparatus in a sternal (sphinx-like) position. The animal's head was inserted into a custom built RF coil and MRI compatible ear inserts, which contained sound attenuating buds and a tube to direct the auditory stimulus close to the tympanic membrane, were placed in each ear. Both sides of the head were stabilized with sound dampening foam padding which aided in the attenuation of scanner noise (Fig. 1). The cat and apparatus were then placed inside the bore of the magnet.

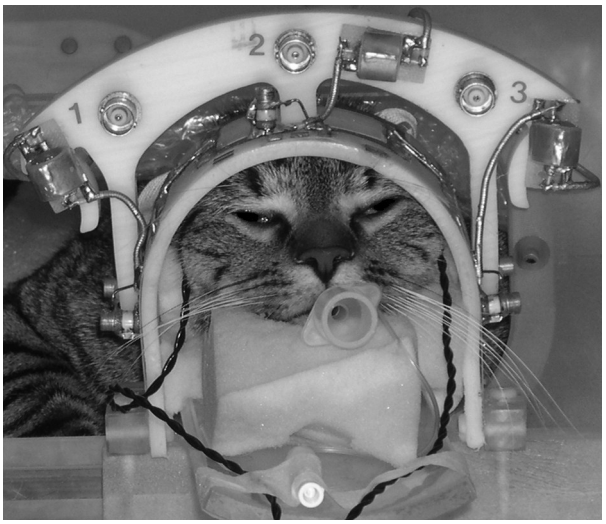

Fig. 1. A photograph of an anesthetized animal in the RF coil. Braided black cords lateral to the animal's head terminate at ear buds inserted into each ear canal. The head is enveloped in foam to minimize movement and attenuate scanner noise. The animal is intubated (plastic tube ventral to nose) to permit administration of isofluorane anesthesia.

Anesthesia was maintained through the continuous administration of ketamine (0.6–0.75 mg/kg/h) intravenous (i.v.) and spontaneous inhalation of iosflurane (0.4–0.5%). In our experience, these levels resulted in the collection of optimal fMRI data. On average, sessions lasted 2 h.

Following each scanning session, anesthesia was discontinued and the cat was monitored closely during recovery. The endotracheal tube was removed when the cat exhibited a gag reflex and increased jaw tone. The catheter remained in place until the cat exhibited voluntary head and limb movement. The cat was then placed in individual housing until fully recovered from the effects of anesthesia at which time it was returned to the clowder. Generally, animals exhibited normal behavior within 1 h of anesthesia cessation.

2.2. Image acquisition

All data were acquired on an actively shielded 68 cm human head 7-T horizontal bore scanner with a DirectDrive console (Agilent, Santa Clara, CA) equipped with a Siemens AC84 gradient subsystem (Erlangen, Germany) operating at a slew rate of 280 mT/m/s. An in-house designed and manufactured conformal 3-channel transceiver cat head RF coil was used for all experiments (Fig. 1). Magnetic field optimization (B0 shimming) was performed using an automated 3D mapping procedure (Klassen and Menon, 2004) over the specific imaging volume of interest.

For each cat, functional volumes were collected using a segmented interleaved EPI acquisition (TR = 1000 ms; TE = 15 ms; 3 segments/plane; slices = 21 mm × 1 mm; matrix = 96 × 96; FOV = 72 mm × 72 mm; acquisition voxel size = 0.75 mm × 0.75 mm × 1.0 mm; acquisition time (TA) = 3 s/volume). Images were corrected for physiological fluctuations using navigator echo correction (Hu and Kim, 1994). A high-resolution PD-weighted anatomical reference volume was acquired along the same orientation and field-of-view as the functional images using a FLASH imaging sequence (TR = 750 ms; TE = 8 ms; matrix = 256 × 256; acquisition voxel size = 281 μm × 281 μm × 1.0 mm). Functional imaging data sets were acquired for both continuous (120 continuous volumes) and sparse (53 volumes with 5 s delay between each volume) scanning paradigms during every session.

2.3. Stimulus presentation

The stimuli, used during both sparse and continuous scanning methods, consisted of a broadband noise (BBN; white noise), a 0.5 kHz tone and a 10 kHz tone. Each was presented, in bursts of 400 ms with a 100 ms interstimulus ("silent") interval, continuously for 4 s or 30 s for the sparse or continuous paradigms, respectively. Stimuli were generated using MatLab (MathWorks) and were presented using in-house custom software (Microsoft Visual Studio) on a Dell laptop through an external Roland Corporation soundcard (24-bit/96 kHz; Model UA-25EX), a PylePro power amplifier (Model PCAU11) and Sensimetrics MRI-compatible ear inserts (Model S14). Sound card and amplifier output levels were the same for all stimuli. Following data collection, speaker level measurements using an Etymotic Probe Microphone (Elk Grove Village, IL) and Tektronix oscilloscope (Beaverton, OR) confirmed presentation of all stimuli at levels 80–95 dB SPL out of the ear inserts.

Both sparse and continuous scanning methods were conducted using a block design of stimulus presentation (Fig. 2A). For sparse scans, a block of 4 volumes (TR = 8 s and TA = 3 s, resulting in a 5 s gap between volume acquisitions) was collected every 32 s (Fig. 2B) and, for continuous scans a block of 10 volumes (TR and TA = 3 s) was collected every 30 s (Fig. 2C). Two blocks for each stimulus type were collected per run interleaved with baseline blocks in which no stimulus was presented. This resulted in a 6.9 or 6.5 min time for a single sparse or continuous run, respectively.

During sparse scanning the following sequence was applied for each block: (i) a 1 s delay occurred after the start of each silent period; (ii) the stimulus was played for 4 s; (iii) volume acquisition began at stimulus offset (Fig. 2B). Presentation of the stimulus for 4 s allowed enough time for the hemodynamic response to peak (Brown et al., 2013) before acquisition and ensured maintenance of a maximal hemodynamic response throughout the acquisition period (3 s). In contrast, the continuous paradigm included constant stimulus presentation during the entire block.

At the beginning of each session, a structural MRI was collected. Basic on-line analysis of activity was faster and provided higher statistical strength in a single run using continuous scanning. Therefore, following the structural scan, 2–3 continuous runs were performed and evaluated for activity. Once acoustically evoked activity was confirmed, sparse scanning commenced. The initial induction of anesthesia uses an alpha-2 agonist, dexdomitor, which has sedative, analgesic, and muscle relaxing effects and takes approximately 1 h to be metabolized. Therefore, at the end of each session several continuous runs were collected to control for the effects of anesthesia. Two sessions with each subject were included in this study. A minimum of 40 volumes per stimulus for continuous and sparse scanning were required for a session to be included.

2.4. Data analysis

fMRI data from each animal was preprocessed and analyzed separately using SPM8 (Wellcome Trust Centre for Neuroimaging, UCL, London, UK) and MatLab (MathWorks) software. Initially, all images were reoriented and motion corrected (all translational and rotational movements were <0.5 mm) and co-registered to the high resolution structural image from the same session. All sessions were then normalized to a single animal's structural image resulting in a 1 mm isotropic voxel size and smoothed using a 2 mm Gaussian full width at half maximum (FWHM) kernel.

Data were analyzed for each animal using a separate model for continuous and sparse scans. The last two runs of continuous data and the last 5 runs of sparse data from each session were included in further analysis. This ensured that volume numbers for both

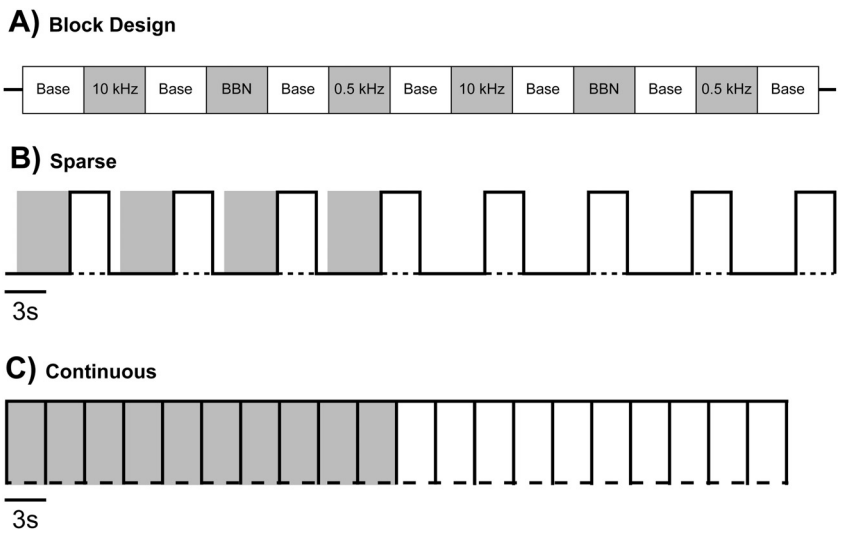

Fig. 2. Schematic of the block design (A) in which stimuli were presented. (B) Two blocks, a stimulus presentation and a baseline, are diagramed for the sparse scanning method. Stimuli are presented during the relatively silent period between acquisitions. Four volumes of data are collected every 32 s using the sparse scanning method. Shading indicates presence of stimuli and the solid line indicates scanner acquisition activity. (C) Two blocks, a stimulus presentation and baseline, are diagramed for the continuous method. Stimuli were presented during acquisition allowing ten volumes of data to be collected every 30 s. Conventions same as in (A).

continuous and sparse scanning, for each stimulus, were equal. Analysis only including the last two runs of sparse data was also included for comparison of time matched runs with continuous data. A correlational AR(1) model was used in conjunction with a high-pass filter of 128 s and restricted maximum likelihood (ReML) model estimation was used (Friston et al., 2007). Following model estimation, a *t*-contrast was generated for each of the stimuli.

Hand drawn region of interest (ROI) masks were generated for auditory cortex, thalamus, and midbrain based on anatomy. These masks were used, in conjunction with small volume correction, to extract time-course data for significantly active voxels associated with each region.

Data from each animal were extracted separately. A voxelwise threshold of $p < 0.001$ (uncorrected) and a cluster-level threshold of $p < 0.05$ (FWE-corrected) were applied to all results. *T*-statistics and percent signal changes (PSC) were examined in order to compare variability and strength of activation. Time courses were extracted for all voxels within a 1 mm radius sphere centered at each peak voxel for further analysis. Average PSC for each volume in a stimulus block was calculated by extracting PSC values for every volume in each block within an individual animal and then averaging across all blocks and animals. One-way analysis of variance (ANOVA) and Tukey's honestly significant difference criteria were then performed to analyze differences between volumes in a block. Data from peak volumes were then extracted and two sample *t*-tests were run to make comparisons between the cortex, thalamus and midbrain activations.

3. Results

Data were inspected for significant activations in the auditory cortex, thalamus or midbrain. Sparse scanning data, time matched to continuous data, resulted in no significant activations. Significant activations were observed in the auditory cortex and midbrain (Fig. 3A and B) in data matched for number of volumes. However, no activations were observed within the thalamus. Magnitude of activation and statistical strength at peak voxels as well as extent of activation were analyzed, across cats, to address differences between sparse and continuous scanning methods within a block. Finally, volumes within a block which elicited the strongest activation were further analyzed for comparison of cortical and midbrain activations.

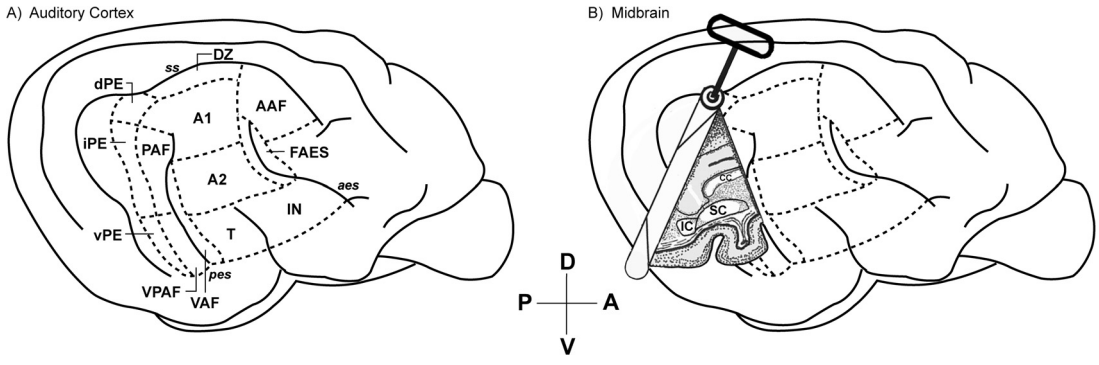

Fig. 3. Activations were observed in the auditory cortex and midbrain. (A) The thirteen cortical areas are indicated: anterior auditory field, AAF; auditory field of the anterior ectosylvian sulcus, FAES; dorsal zone of the auditory cortex, DZ; insular region, IN; posterior auditory field, PAF; primary auditory cortex, A1; second auditory cortex, A2; temporal region, T; ventral auditory field, VAF; ventral posterior auditory field, VPAF; dorsal posterior ectosylvian area, dPE; intermediate posterior ectosylvian area, iPE; ventral posterior ectosylvian area, vPE. Sulci are indicated by italics: anterior ectosylvian sulcus, aes; posterior ectosylvian sulcus, pes; suprasylvian sulcus, ss. (B) Subcortical structures are indicated: superior colliculus (SC); inferior colliculus (IC); and corpus callosum (cc). Anterior (A), posterior (P), dorsal (D) and ventral (V) directions are indicated.

3.1. Cortical activations

The auditory cortex of the cat lies on the lateral surface of the cerebrum and is functionally divided into 13 acoustically responsive areas (Fig. 3A). Activations within auditory cortex were observed through the full thickness of cortex for both continuous (Fig. 4A) and sparse (Fig. 4B) scanning methods. Peak voxels within clusters passing an FWE threshold of $p < 0.05$ did not show a significant difference in statistical strength between sparse and continuous scanning for either the BBN or 0.5 kHz tone (Fig. 4C). The 10 kHz tone did not elicit a response during sparse scanning, and was only effective in two animals during continuous scanning, prohibiting a comparison between the two methods using this stimulus. Therefore, data are not shown for the 10 kHz tone.

Continuous scanning resulted in a significantly larger extent of activation for both the BBN and 0.5 kHz stimuli (Fig. 4D). This is also reflected in the number of peaks resulting from continuous scanning in each individual area (Table 1). Within each cortical area, a larger number of peaks resulting from the 0.5 kHz tone were found within known tonotopic areas such as the primary auditory cortex (A1), the posterior auditory field (PAF) and the ventral posterior auditory field (VPAF; Table 1). Conversely, the BBN resulted in a larger number of peaks appearing within non-tonotopically organized auditory cortices such as the second auditory cortex (A2), dorsal zone (DZ), insular (IN), ventral posterior ectosylvian gyrus (vPE), temporal (T) and ventral auditory field (VAF). While both continuous and sparse scanning demonstrated these organizational principles, it was more apparent using continuous as a result of the larger number of peaks.

3.2. Midbrain activations

Midbrain structures, including the superior and inferior colliculi, lie deep within the brain (Fig. 3B). Activations were identified in the midbrain using both continuous (Fig. 5A) and sparse (Fig. 5B) scanning methods. The data tended to be lateralized to either the right or the left using continuous scanning. Three of the animals had a bias to the left and one a bias to the right. No significant difference was observed for statistical strength (Fig. 5C) or extent of activation (Fig. 5D) between continuous and sparse scanning.

3.3. Hemodynamic response

The difference in the stimulation sequence between continuous and sparse scanning, namely that the stimulus is presented continuously for 4 s during sparse scanning and for 30 s during continuous runs, could bias results. When considering the time from stimulus onset, the second volume of the continuous block (3–6 s) best matches the first volume of the sparse block (4–7 s). Analysis of these volumes separately showed no significant difference in the percent signal change (PSC) between continuous and sparse scanning in cortex (Fig. 6A) or midbrain for either BBN or 0.5 kHz stimuli (Fig. 6B). There was also no difference between the last volumes of the continuous and sparse blocks.

However, in cortex there was a significant increase in PSC between the second volume and the last volume of the continuous block for both stimuli (Fig. 6A). A similar pattern was also seen for sparse scanning, having a significant increase in PSC in the last volume of the block during stimulation with a 0.5 kHz tone. A comparable difference was also observed in the midbrain activations using sparse scanning during 0.5 kHz stimulation.

Average PSC for each acquired volume within a block better illustrates the increasing trend for cortex (Fig. 7A) and midbrain (Fig. 7B). Cortical activations following the second volume show a significant increase in PSC during continuous scanning (Fig. 7Ai). Conversely, activations in the midbrain during

Table 1
Number of peaks found within each of the cortical areas.

	A1		AAF		PAF		VPAF		DZ		A2		IN		VPE		T		VAF		Total
	BBN	0.5	BBN	0.5	BBN	0.5	BBN	0.5	BBN	0.5	BBN	0.5	BBN	0.5	BBN	0.5	BBN	0.5	BBN	0.5	
Continuous	4	7	1	0	0	0	0	1	5	3	4	1	2	2	1	0	1	0	4	1	37
Sparse	2	1	0	0	0	2	0	1	2	1	2	0	2	0	0	0	0	0	3	0	16

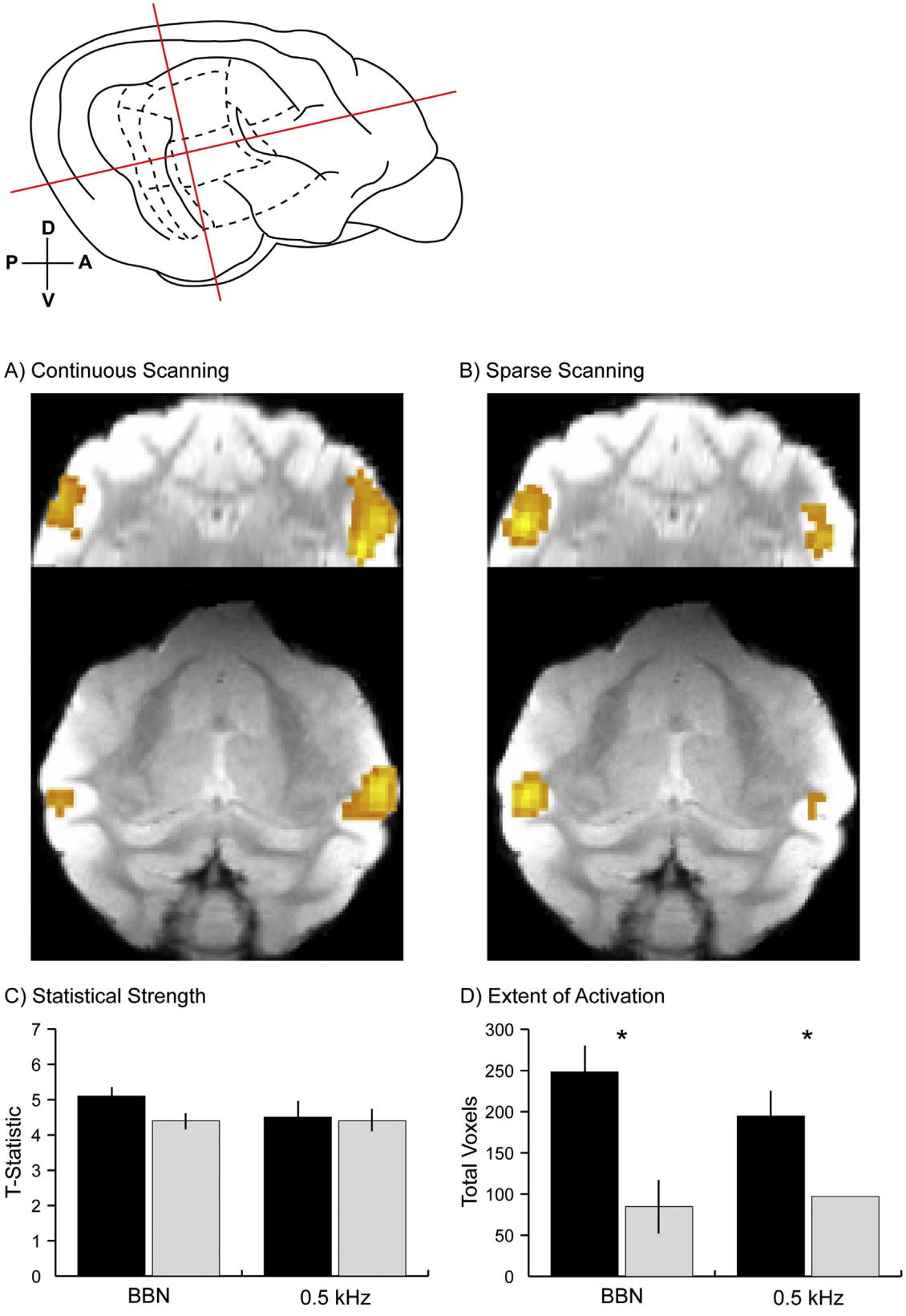

Fig. 4. Activations within auditory cortex. (A and B) Cortical activations, in a single animal in response to BBN, for continuous (A) or sparse (B) scanning methods. Cortical representation at top shows locations of coronal and horizontal slices shown in (A) and (B). Activations passed $p < 0.001$ uncorrected and cluster FWE thresholds. (C) Average t-statistics at peak voxels within cortical activations are indicated for continuous (black bars) and sparse (gray bars) scanning. (D) Extent of activation across cortex. Number of active voxels are indicated for continuous (black bars) and sparse (gray bars) scanning. Error bars represent S.E.M. * indicates $p < 0.01$.

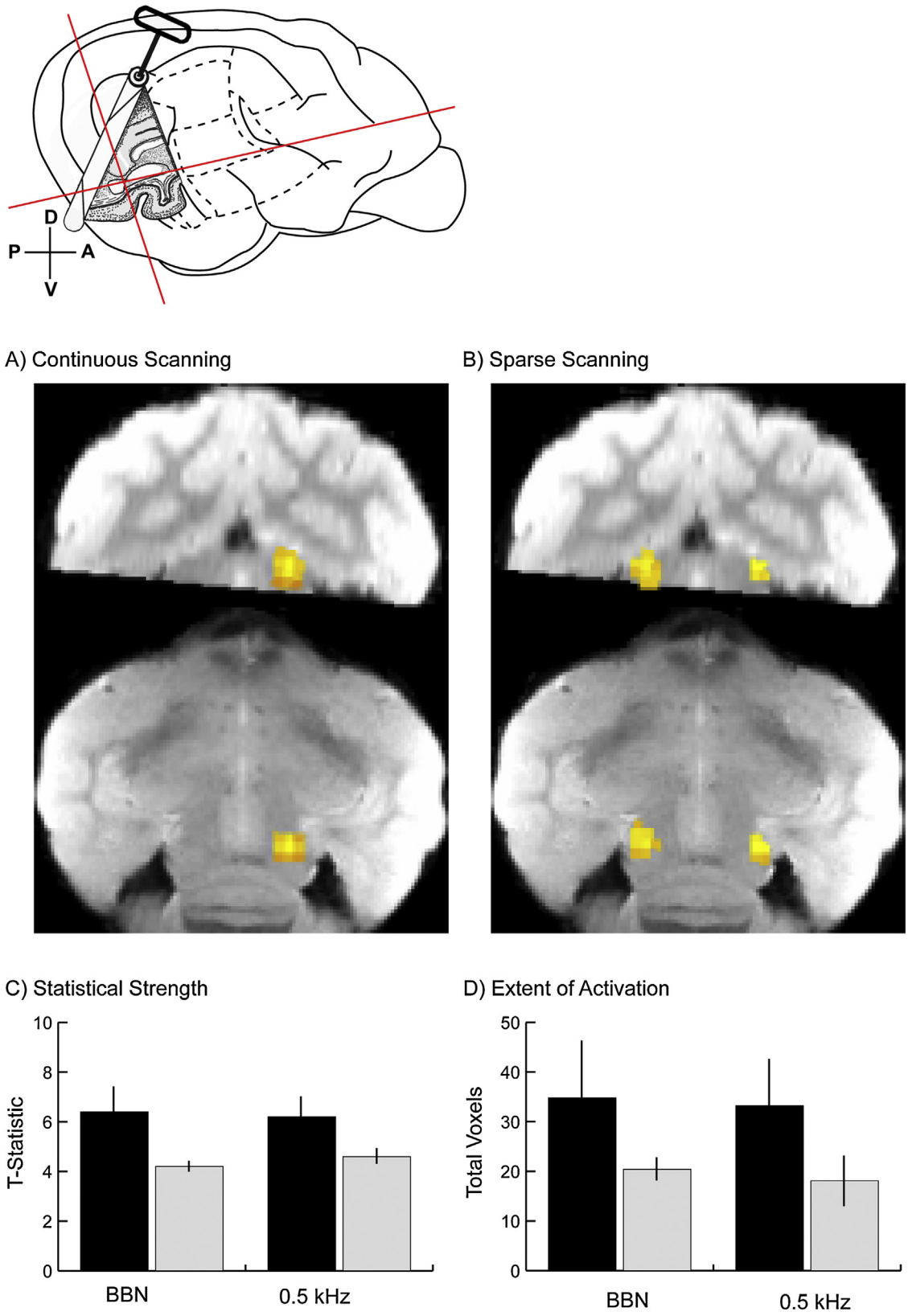

Fig. 5. Activations in the midbrain. (A and B) Midbrain activations, in a single animal in response to 0.5 kHz tone, for continuous (A) or sparse (B) scanning methods. Subcortical representation at top shows locations of coronal and horizontal slices shown in (A) and (B). Activations passed $p < 0.001$ uncorrected and cluster FWE thresholds. (C) Average *t*-statistics at peak voxels within midbrain activations are indicated for continuous (black bars) and sparse (gray bars) scanning. (D) Extent of activation across the midbrain. Number of active voxels are indicated for continuous (black bars) and sparse (gray bars) scanning. Error bars represent S.E.M. * indicates $p < 0.01$.

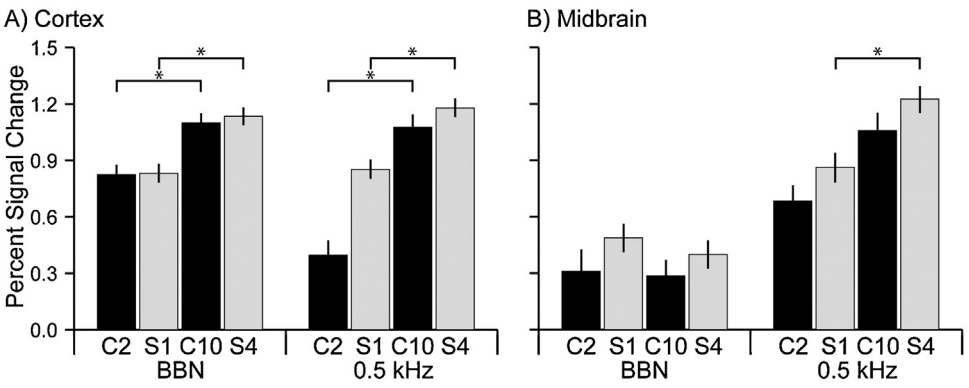

Fig. 6. Stimulus presentation was not identical between continuous and sparse scanning. The second volume of the continuous runs (C2), an approximate time match for stimulus presentation to the first volume of the sparse runs (S1), is shown for both cortical (A) and midbrain (B) activations. The last volume for the continuous (C10) and sparse (S4) runs are also shown. Error bars represent S.E.M. * indicates $p < 0.01$.

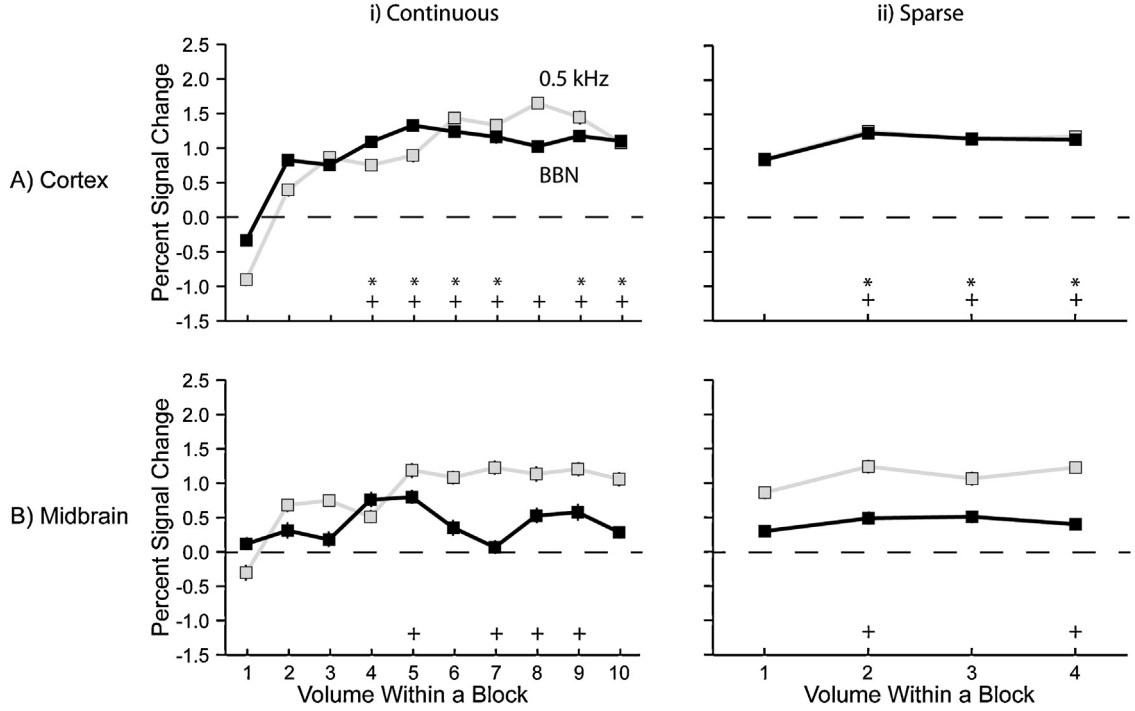

Fig. 7. Hemodynamic time course. Mean percent signal change (PSC) in peak voxels for each volume in cortex (A) or midbrain (B) for both BBN (black lines) and 0.5 kHz (gray lines). (i) Continuous scanning, significant differences from the second volume are indicated for both BBN (*) and 0.5 kHz (+). (ii) Sparse scanning, significant differences from the first volume for both BBN (*) and 0.5 kHz (+) are indicated. Error bars represent S.E.M. * or + indicates $p < 0.01$.

continuous scanning (Fig. 7Bi) were, with a few exceptions during stimulation with the 0.5 kHz tone, generally not significantly different from the second volume. During sparse scanning, the timing of the stimulus onset was precisely placed so that each acquisition would be sampling at the peak of the hemodynamic response and was expected to result in a fairly flat PSC across a block. It is intriguing that data indicate that cortical activations during sparse scanning (Fig. 7Aii) also showed an upward trend through the block. Midbrain activations during sparse scanning (Fig. 7Bii) using the BBN more closely reflected the flat PSC across the block as was expected. However, midbrain activations during sparse scanning using the 0.5 kHz tone showed significantly higher PSC for two volumes, compared to the first.

3.4. Cortical and midbrain comparison

Time courses of volumes within a block eliciting the strongest activation (Fig. 7) were then compared for midbrain and cortical activations for each scanning method. The PSC at these peak volumes was significantly lower for midbrain activations during continuous scanning during presentation of each stimulus (Fig. 8A). Similarly, during sparse scanning (Fig. 8B), midbrain activations were significantly lower for the BBN stimulus. There were, however, no significant differences between cortical and midbrain activations using the 0.5 kHz stimulus during sparse scanning.

4. Discussion

In summary, activations of auditory cortex and midbrain structures resulted in similar statistical strengths and magnitudes for both continuous and sparse scanning. The differences between the two methods are best demonstrated in extent and location of cortical activation. Also, a rise in magnitude of activation was observed along a block for both continuous and sparse scanning. Finally, midbrain activations had significantly lower magnitude compared to cortical activations.

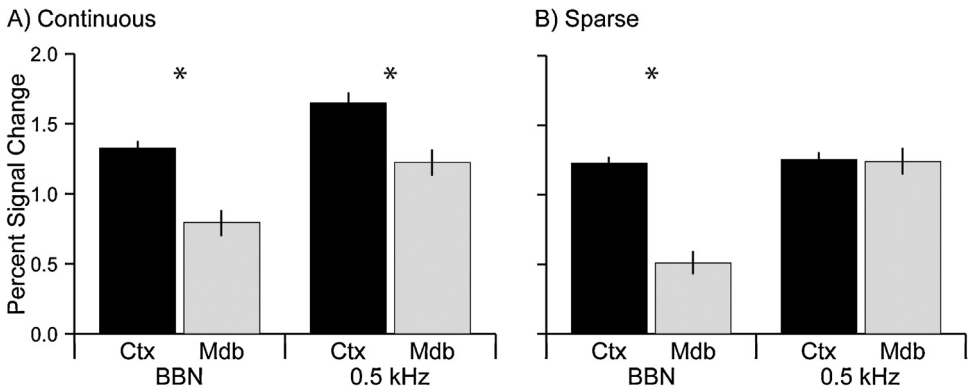

Fig. 8. Comparison of cortical and midbrain activations. (A) Activations at peak volumes and voxels for both cortex and midbrain using the continuous scanning method. (B) Activations at peak volumes and voxels for both cortex and midbrain using the sparse scanning method. Error bars represent S.E.M. * indicates $p < 0.01$.

4.1. Continuous versus sparse scanning

The common use of sparse scanning in current fMRI investigations of acoustically evoked activity would suggest that it is superior to the more traditional continuous method. In fact, previous human and non-human primate studies which have directly compared the two techniques, have indicated that sparse scanning resulted in larger magnitude and extent of activation (Hall et al., 1999; Peelle et al., 2010; Petkov et al., 2009; Schmidt et al., 2008; Woods et al., 2009). In contrast, results from the present study showed no difference in magnitude of activation between the two methods (Figs. 6 and 7) and a significantly higher extent of cortical activation (Fig. 4D) using the continuous method. Variations between these studies and the present one could be attributed to differences in acquisition (Petkov et al., 2009), volume sampling (Hall et al., 1999), or stimulus presentation timing (Schmidt et al., 2008). For example, Petkov et al. (2009) increased the acquisition time during continuous scanning in an attempt to temporally equalize the two methods. This may have introduced a greater degree of variability into each volume of continuous as a result of physiological movements, such as respiration or heartbeat, than was present in volumes acquired using sparse scanning. This could result in masking of neural-based BOLD responses by artifact induced by such movements.

Previous studies have also noted better statistics using continuous scanning. Results from the present study did not find a significant difference in statistical power. However, to generate the fairest comparison between the two techniques, the number of volumes included in the analysis was equalized. One of the benefits of continuous scanning is the ability to collect larger amounts of data in a similar time frame. Taking into account time constraints, which are normally a factor in studies using fMRI, the larger amount of data which can be collected in the same amount of time would enhance statistical power using continuous scanning.

Previous work using continuous scanning has also resulted in similar, if not better, demonstrations of organizational principles such as primary versus non-primary cortex (Petkov et al., 2009) and functional maps (Woods et al., 2009). In agreement with previous studies, the present results show a better functional mapping of auditory cortex using continuous scanning. Cortical areas, such as A1, which are known to be tonotopic (Imig and Reale, 1980; Reale and Imig, 1980) show a larger number of peaks, using both continuous and sparse scanning, during tonal stimulation. Conversely, areas outside of primary auditory cortex show a larger number of peaks in response to BBN stimulation using both methods. However, this effect is magnified using continuous scanning, resulting in a larger number of peaks as well as peaks in areas that were not identified using sparse such as vPE and T.

The amplified laterality of activations using continuous, as opposed to sparse, scanning was surprising. It is well known, in humans, that there is a lateral weighting of acoustic activation, especially in response to language. However, the present investigation did not involve vocalizations, human or conspecific, and for this laterality to be exaggerated in continuous scanning was not expected. The two paradigms, used during the present investigation, differed in their stimulus duration. During sparse scanning, the stimulus was presented for 4 s while it was presented for a full 30 s during continuous scanning. Zaehle et al. (2004) found that there is a laterality associated with both tone and temporal changes, such as gap detection and information processing. The difference in the stimulation paradigms may provide an explanation not only for the existence of the laterality, but also for the differences in the laterality between the two methods.

In addition to the benefits of continuous over sparse scanning in volume matched data, time matched data also indicates continuous as the optimal method for fMRI in the cat using a 7 T, high field, scanner. Using the same number of runs, meaning less data included for sparse scanning, resulted in no significant activations observed using sparse scanning. This indicates that in the same amount of time sparse scanning may not be able to collect enough data to be usable.

4.2. Duty cycle

Length of stimulus presentation, or duty cycle, has been shown to affect both neural and hemodynamic responses (Birn and Bandettini, 2005; Eggermont, 1994). Therefore, differences noted between the two paradigms, in the present study, could have been a result of stimulation differences. Birn and Bandettini (2005) noted that the effects of duty cycle are most pronounced for stimuli which have durations less than 2 s. Stimulus lengths in this study were both $\geq$4 s. Therefore, effects of duty cycle were expected to be minimal. In the continuous run, the second volume starts 3 s after stimulation begins and ends at 6 s. This is the closest match to the sparse volumes which started 4 s after stimulation begins and ends at 7 s. If the duty cycle phenomenon was affecting the present data then the second volume of the continuous block and first volume of the sparse block should have been similar while the last volumes were different. Both comparisons were statistically the same (Fig. 6) and therefore effects of duty cycle were not observed in the present study.

4.3. Auditory pathway activations

A few studies have investigated BOLD responses at different stages of the auditory pathway in humans. Baumann et al. (2010)

found similar time courses for the inferior colliculus (IC) and auditory cortex (AC) peaking at approximately 4 s. The time course of the medial geniculate body (MGB) of the thalamus however was slightly later peaking at approximately 5 s. This study also noted that AC has the highest percent signal change in relation to IC and MGB activation. Also, with few exceptions, the IC has higher percent signal change than MGB. Similarly Backes and van Dijk (2002) found no difference in the HRF time courses of the IC and AC. However, this study noted that in many of their subjects MGB activations were not identified. They also noted no significant difference in the percent signal change between IC and AC activations. In rats, Cheung et al. (2012) found that activations in subcortical regions were more robust than those in AC. However, this can be attributed to use of high levels of isofluorane as anesthesia which has been shown to alter cortical responsiveness to auditory stimuli (Cheung et al., 2001).

The poorer strength of significant thalamic activation observed during this investigation was not surprising given similar results in previous studies (Backes and van Dijk, 2002; Baumann et al., 2010). It is however, interesting that MGB activations were observed using continuous scanning while no significant activations could be elicited using sparse scanning. We can postulate that the timing of the volume collection along the HRF is most likely the culprit for this discrepancy. Currently there has not been an investigation published on the HRF of the MGB in the cat using fMRI. However, Baumann et al. (2010) found that the HRF peak for the MGB occurred later than AC and IC activations in non-human primates. If this were true than the start of volume acquisition during sparse scanning, in the present investigation, was not optimally timed for capturing activations of the MGB.

The present investigation resulted in higher percent signal change in AC when compared to IC. The increased activation within AC could be a product of a couple factors: (1) vascularization differences and (2) neuronal processing differences. It has been noted that regions with larger capillary densities result in higher cerebral blood flow (Gerrits et al., 2000; Harrison et al., 2002; Song et al., 2011). The central nucleus of the IC is most likely the largest part of the activations observed in the present study since its microvascularization is significantly larger than the lateral and dorsal cortex of the IC (Song et al., 2011). The lack of MGB activation may be due to vascularization differences since it has lower recorded glucose utilization and blood flow (Baumann et al., 2010). No current literature directly compares capillary densities of AC and IC. Therefore, further investigation would be necessary to determine if the vascularization is causing the differences seen in the present study. As noted previously, the central nucleus of the IC is most likely driving the activations seen in the present study because it is more vascular than the other two divisions of IC (Song et al., 2011). This nucleus receives mostly afferent projections, projects to the ventral MGB, and is tonotopic (Malmierca and Hackett, 2010; Schreiner and Langner, 1997). It is not surprising then that IC activation was more robust with tonal stimulation. Auditory cortex on the other hand is quite expansive comparatively. A few regions within AC are tonotopic but the majority of AC is not. This explains why activation in response to BBN was so much more robust in cortex (Fig. 8). Also, AC receives ascending input as well as lateral or descending input from other cortical areas and divisions of the MGB. This would result in heightened activity levels within AC and cause the larger percent signal change in AC compared to the IC.

5. Conclusions

In the present study we have successfully demonstrated that activations within the midbrain and cortex can be revealed using both fMRI techniques. When volume numbers were equalized, the extent of activation was larger using continuous scanning and resulted in a greater number of peaks. Also, it is likely that statistical power would also be greater for continuous scanning given the added benefit of more volumes in the same amount of time. Therefore, we conclude that, during passive stimulation in an anesthetized animal, continuous scanning is the preferred method for investigations of auditory cortex in the cat using fMRI. Also, choice of method for future investigations of midbrain activity should be driven by other experimental factors, such as stimulus intensity and task performance during scanning given no significant differences in activation exist between the two methods.

Acknowledgements

The authors would like to acknowledge the contributions of Kyle Gilbert, who designed the custom RF coil, and Kevin Barker, who designed the apparatus supporting the animals. This work was supported by the Canadian Institutes of Health Research (CIHR), Natural Sciences and Engineering Research Council of Canada (NSERC), and Canada Foundation for Innovation (CFI).

References

Amaro E, Williams SCR, Shergill SS, Fu CHY, MacSweeney M, Picchioni MM, et al. Acoustic noise and functional magnetic resonance imaging: current strategies and future prospects. J Magn Reson Imaging 2002;16:497–510.
Backes WH, van Dijk P. Simultaneous sampling of event-related BOLD responses in auditory cortex and brainstem. Magn Reson Med 2002;47:90–6.
Bandettini PA, Jesmanowicz A, Van Kylen J, Birn RM, Hyde JS. Functional MRI of brain activation induced by scanner acoustic noise. Magn Reson Med 1998;39:410–6.
Baumann S, Griffiths TD, Rees A, Hunter D, Sun L, Thiele A. Characterisation of the BOLD response time course at different levels of the auditory pathway in non-human primates. Neuroimage 2010;50:1099–108.
Belin P, Zatorre RJ, Hoge R, Evans AC, Pike B. Event-related fMRI of the auditory cortex. Neuroimage 1999;10:417–29.
Birn RM, Bandettini PA. The effect of stimulus duty cycle and off duration on BOLD response linearity. Neuroimage 2005;27:70–82.
Brown TA, Joanisse MF, Gati JS, Hughes SM, Nixon PL, Menon RS, et al. Characterisation of the BOLD response in cat auditory cortex. Neuroimage 2013;64:458–65.
Cheung MM, Lau C, Zhou IY, Chan KC, Cheng JS, Zhang JW, et al. BOLD fMRI investigation of the rat auditory pathway and tonotopic organization. Neuroimage 2012;60:1205–11.
Cheung SW, Nagarajan SS, Bedenbaugh PH, Schreiner CE, Wang XQ, Wong A. Auditory cortical neuron response differences under isoflurane versus pentobarbital anesthesia. Hear Res 2001;156:115–27.
Davis MH, Johnsrude IS. Hierarchical processing in spoken language comprehension. J Neurosci 2003;23:3423–31.
Dyson DH, Allen DG, Ingwersen W, Pascoe PJ. Evaluation of acepromazine meperidine atropine premedication followed by thiopental anesthesia in the cat. Can J Vet Res 1988;52:419–22.
Edmister WB, Talavage TM, Ledden PJ, Weisskoff RM. Improved auditory cortex imaging using clustered volume acquisitions. Hum Brain Mapp 1999;7:89–97.
Eggermont JJ. Temporal modulation transfer functions for AM and FM stimuli in cat auditory cortex. Effects of carrier type, modulating waveform and intensity. Hear Res 1994;74:51–66.
Friston KJ, Ashburner J, Kiebel SJ, Nichols TE, Penny WD, editors. Statistical parametric mapping: the analysis of functional brain images. Boston: Academic Press; 2007.
Gerrits RJ, Raczynski C, Greene AS, Stein EA. Regional cerebral blood flow responses to variable frequency whisker stimulation: an autoradiographic analysis. Brain Res 2000;864:205–12.
Hall DA, Haggard MP, Akeroyd MA, Palmer AR, Summerfield AQ, Elliott MR, et al. Sparse temporal sampling in auditory fMRI. Hum Brain Mapp 1999;7:213–23.
Harrison RV, Harel N, Panesar J, Mount RJ. Blood capillary distribution correlates with hemodynamic-based functional imaging in cerebral cortex. Cereb Cortex 2002;12:225–33.
Hu XP, Kim SG. Reduction of signal fluctuation in functional MRI using navigator echoes. Magn Reson Med 1994;31:495–503.
Imig TJ, Reale RA. Pattern of cortico-cortical connections related to tonotopic maps in cat auditory-cortex. J Comp Neurol 1980;192:293–332.
Inan S, Mitchell T, Song A, Bizzell J, Belger A. Hemodynamic correlates of stimulus repetition in the visual and auditory cortices: an fMRI study. Neuroimage 2004;21:886–93.
Klassen LM, Menon RS. Robust automated shimming technique using arbitrary mapping acquisition parameters (RASTAMAP). Magn Reson Med 2004;51:881–7.
Langers DRM, Backes WH, van Dijk P. Representation of lateralization and tonotopy in primary versus secondary human auditory cortex. Neuroimage 2007;34:264–73.

Malmierca MS, Hackett TA. Structural organization of the ascending auditory pathway. In: Moore DR, editor. The Oxford handbook of auditory science: the auditory brain. Oxford: Oxford University Press; 2010. p. 9–42.
Moelker A, Pattynama PMT. Acoustic noise concerns in functional magnetic resonance imaging. Hum Brain Mapp 2003;20:123–41.
Olfert ED, Cross BM, McWilliam AA. Guide to the care and use of experimental animals. Canadian Council on Animal Care; 1993.
Peelle JE, Eason RJ, Schmitter S, Schwarzbauer C, Davis MH. Evaluating an acoustically quiet EPI sequence for use in fMRI studies of speech and auditory processing. Neuroimage 2010;52:1410–9.
Petkov CI, Kayser C, Augath M, Logothetis NK. Optimizing the imaging of the monkey auditory cortex: sparse vs. continuous fMRI. J Magn Reson Imaging 2009;27:1065–73.
Price DL, De Wilde JP, Papadaki AM, Curran JS, Kitney RI. Investigation of acoustic noise on 15 MRI scanners from 0.2 T to 3 T. J Magn Reson Imaging 2001;13:288–93.
Ravicz ME, Melcher JR, Kiang NYS. Acoustic noise during functional magnetic resonance imaging. J Acoust Soc Am 2000;108:1683–96.
Reale RA, Imig TJ. Tonotopic organization in auditory cortex of the cat. J Comp Neurol 1980;192:265–91.
Scarff CJ, Reynolds A, Goodyear BG, Ponton CW, Dort JC, Eggermont JJ. Simultaneous 3-T fMRI and high-density recording of human auditory evoked potentials. Neuroimage 2004;23:1129–42.
Schmidt CF, Zaehle T, Meyer M, Geiser E, Boesiger P, Jancke L. Silent and continuous fMRI scanning differentially modulate activation in an auditory language comprehension task. Hum Brain Mapp 2008;29:46–56.
Schreiner CE, Langner G. Laminar fine structure of frequency organization in auditory midbrain. Nature 1997;388:383–6.
Song Y, Mellott JG, Winer JA. Microvascular organization of the cat inferior colliculus. Hear Res 2011;274:5–12.
Talavage TM, Edmister WB, Ledden PJ, Weisskoff RM. Quantitative assessment of auditory cortex responses induced by imager acoustic noise. Hum Brain Mapp 1999;7:79–88.
Talavage TM, Ledden PJ, Benson RR, Rosen BR, Melcher JR. Frequency-dependent responses exhibited by multiple regions in human auditory cortex. Hear Res 2000;150:225–44.
van den Noort M, Specht K, Rimol LM, Ersland L, Hugdahl K. A new verbal reports fMRI dichotic listening paradigm for studies of hemispheric asymmetry. Neuroimage 2008;40:902–11.
Van Sluyters RC, Ballinger M, Bayne K, Cunningham C, Degryse A-D, Dubner R, et al. Guidelines for the care and use of mammals in neuroscience and behavioral research. Washington, DC: National Research Council; 2003.
Vannest JJ, Karunanayaka PR, Altaye M, Schmithorst VJ, Plante EM, Eaton KJ, et al. Comparison of fMRI data from passive listening and active-response story processing tasks in children. J Magn Reson Imaging 2009;29:971–6.
Wessinger CM, Buonocore MH, Kussmaul CL, Mangun GR. Tonotopy in human auditory cortex examined with functional magnetic resonance imaging. Hum Brain Mapp 1997;5:18–25.
Woods DL, Stecker GC, Rinne T, Herron TJ, Cate AD, Yund EW, et al. Functional maps of human auditory cortex: effects of acoustic features and attention. PLoS ONE 2009;4:e5183.
Zaehle T, Wustenberg T, Meyer M, Jancke L. Evidence for rapid auditory perception as the foundation of speech processing: a sparse temporal sampling fMRI study. Eur J Neurosci 2004;20:2447–56.